Desalination and Water Treatment
www.deswater.com

doi: 10.5004/dwt.2019.23180

137 (2019) 134–142
January

A comparison study of granular activated carbon modification by $FeCl_3$ under the acidic and basic condition for arsenic removal from water

Mokhtar Mahdavi[a,b], Amir Hossein Mahvi[c], Ali Fatehizadeh[d], Mohsen Sadani[e], Behzad Shahmoradi[f], Afshin Ebrahimi[d,g,*]

[a]*Environmental Health Engineering and Student Research Committee, Saveh University of Medical Sciences, Saveh, Iran, email: ShamaLL6@yahoo.com*
[b]*Social Determinants of Health Research Center, Saveh University of Medical Sciences, Saveh, Iran*
[c]*Center for Solid Waste Research, Institute for Environmental Research, Tehran University of Medical Science, Tehran, Iran, email: ahmahvi@yahoo.com*
[d]*Environment Research Center, Research Institute for Primordial Prevention of Non-Communicable Disease, Isfahan University of Medical Sciences, Isfahan, Iran*
[e]*Department of Environmental Health Engineering, School of Public Health, Shahid Beheshti University of Medical Sciences, Tehran, Iran*
[f]*Environmental Health Research Center, Kurdistan University of Medical Sciences, Sanandaj, Iran, email: Iran.bshahmorady@gmail.com*
[g]*Department of Environmental Health Engineering, School of Health, Isfahan University of Medical Sciences, Isfahan, Iran, Tel. +98 3 137923280; email: a_ebrahimi@hlth.mui.ac.ir*

Received 26 January 2018; Accepted 22 September 2018

ABSTRACT

The present study deals with the effect of two different conditions for modification of raw granular activated carbon (GAC) with $FeCl_3$ under acidic granular activated carbon (AGAC) and basic granular activated carbon (BGAC) conditions for removal of arsenic – As(V) – from aqueous solution. X-ray diffraction, scanning electron microscopy, and Brunauer–Emmett–Teller (BET) were used for structural properties. Obtained images show that for raw GAC most of the peaks are related to SiO_2 and graphite, but, for AGAC related to Fe_2O_3, Fe_3O_4, and SiO_2, and for BGAC related to Fe_3O_4 and hydrogen aluminum silicate. Surface area and total pore volume of raw GAC > AGAC > BGAC. Kinetics study for arsenic removal by raw GAC and BGAC obeyed pseudo-first-order model, but, AGAC obeyed pseudo-second-order model. Isotherm study showed that raw GAC has a good fit with Langmuir model, and AGAC and BGAC have a good fit with Freundlich model. The adsorption capacity of AGAC, BGAC, and raw GAC (As(V) concentration = 0.3 mg/L) was 22.7, 18.33, and 14.35 mg/g, respectively. It was concluded that modified raw GAC under the acidic condition had better than basic condition.

Keywords: GAC; Modified GAC; Arsenic removal; Adsorption; Iron oxide/GAC

1. Introduction

One of the most important problems for water resources in many areas of the world is heavy metals contamination. Arsenic is a metalloid that endangers human health. It can cause skin, liver, kidney, and bladder cancers, hyperkeratosis, blackfoot, and melanosis [1,2]. The world health organization (WHO) guideline for arsenic content in drinking water is 0.01 mg/L [3]. Water contamination by arsenic resulted from two ways. First, related to anthropogenic resources such as industrial (electronics, dyes, wood preservatives, pesticides, fertilizers, oil, and solvent product) and agricultural activities [4–6]. The later relates to natural ore and geological properties of soil.

---

* Corresponding author.

There are different methods that have been used for arsenic removal from water and wastewater such as membrane technology [7,8], adsorption by various adsorbents [9–12], application of some media in sand filter [13], electrocoagulation [14], ion exchange or resins [15], and chemical coagulation [16,17]. Each of them has advantages and disadvantages that affect their applications. However, adsorption process has some advantages such as minimal sludge production, specific selection, high removal efficiency, simple to use and low economical cost. So, it has become a favorable method in world [18,19].

There are many studies that have been conducted on arsenic removal by different adsorbents such as Dolomite [20] and activated carbon (AC) produced from low cost materials. During recent years, many researchers have been turning to the modified activated carbon to attain better results. However, this action has been conducted under different conditions including oxidation, coating, and condition such as different temperature, acidic or basic pH [21–23]. Many researchers claimed that Fe coating of AC was ineffective by $FeCl_3$ under very acid solutions ($pH < 1.0$) [23]. On the other hand, some claimed that Fe coating of AC under high concentration of HCl (3 M) and low pH ($pH < 0$), significantly increased the amount of adsorbed iron on it which subsequently, increases arsenic removal [24]. Two described ideas were conducted at different condition including Fe coating methodology, preparation, and also arsenic concentration. The present study describes the influence of acid oxidation, coating of granulated activated carbon (GAC) by $FeCl_3$ under two different pH conditions of acidic ($pH < 0.1$) and basic ($pH > 12$) condition and also, heating of coated GAC for better Fe coating on GAC, and subsequent determination of the best method for arsenate removal.

2. Materials and methods

In this study, the removal of arsenic (arsenate) from water was carried out by raw GAC and chemically modified GAC, supplied by Merck Company's representative in Iran.

2.1. Materials

Analytical grade ferric chloride ($FeCl_3{\cdot}6H_20$), GAC, sulfuric acid, nitric acid, and sodium hydroxide were purchased from Merck Company, Iran. Also, $Na_2HASO_4{\cdot}7H_2O$ was purchased from Sigma-Aldrich Company's representative in Iran.

2.2. Stock solutions of arsenate

As(V) stock solutions were prepared by dissolving accurate amounts of $Na_2HASO_4{\cdot}7H_2O$ in deionized water to produce stock solutions of 1,000 mg/L. Appropriate dilutions were made to give a range of arsenic concentrations of 0.3, 1.2, and 2.15 mg/L.

2.3. Oxidation of GAC

In this study, the oxidation of GAC was conducted by combination of 65% nitric acid and concentrated sulfuric acid [25]. First, 200 g of raw GAC was washed by distilled water several times. Then it was dried at 110°C for 24 h. Forty grams of dried GAC were put in conical flasks then 100 mL of 65% nitric acid and 100 mL of concentrated sulfuric acid were added to it. After that, the solution was mixed in a rotary shaker at 80 rpm for 1 h. Finally, GAC was filtered and separated from acids, washed and stayed in the distilled water for 8 h. Then, GAC was dried at 110°C during 24 h. After these processes, the raw and oxidized GAC were grinded and those with sizes 120 mesh (0.125 mm) used for Fe coating.

2.4. Iron doping of GAC

- Forty grams of the oxidized GAC were mixed with 200 mL of $FeCl_3{\cdot}6H_2O$ solution containing 2.5% of Fe^{3+} and then pH was adjusted to 12 by the addition of 1 N NaOH solution. The impregnation of Fe was carried out at 80°C for 24 h on a shaker with 150 rpm rotation [26]. After that, residual mixture (the impregnated GAC) was calcined at 300°C under N_2 atmosphere for 3 h. Then, it was washed with distilled water for several times and dried at 110°C for 24 h [27]. This GAC, which was oxidized by a mixture of acid and coated by Fe under the basic condition and calcined at 300°C, was named as basic granular activated carbon (BGAC) in this paper.
- Forty grams of the oxidized GAC were mixed with 200 mL of $FeCl_3{\cdot}6H_2O$ solution containing 2.5% of Fe^{3+} and pH was adjusted to <0.3 by the addition of 1 HCl 3M solution [24]. The impregnation of Fe was carried out at 80°C for 24 h on a shaker with 150 rpm rotation. After that residual mixture (the impregnated GAC) was calcined at 300°C under N_2 atmosphere for 3 h. Then, it was washed with distilled water for several times and dried at 110°C for 24 h. This GAC that oxidized by a mixture of acid and coated by Fe under acidic condition and calcined at 300°C was named as acidic granular activated carbon (AGAC), in this paper. Also, raw GAC is GAC without any oxidation and impregnation with $FeCl_3$ which is nominated raw granular activated carbon (RGAC), in this paper (Fig. 1).

2.5. Iron content in raw and modified GAC

The amount of impregnated iron in raw and modified GAC was evaluated according to modified acid extraction method that used by Chang et al. [29]. Three hundred milligrams of raw and modified GAC (GAC, AGAC, and BGAC) were added separately into the 40-mL vials containing 30 mL of 1:1 HCl solution and were shaken for 10 h. Then, they were placed in a water bath at 70°C–80°C for 4 h. After these steps, adsorbents were separated from the solution by GF/C filter paper. Finally, the iron concentrations of separated adsorbents were analyzed by phenanthroline method with Hach spectrophotometer DR5000. The iron content was calculated according to below equation:

$$\text{Iron content} = \frac{\text{Mass of iron}}{\text{Mass of GAC} + \text{Mass of iron}} \times 100 \tag{1}$$

2.6. Adsorption experiments

Adsorption experiments were conducted by batch method (Fig. 2). Experiments included determination of optimum pH, equilibrium time, adsorbents dosage, arsenic

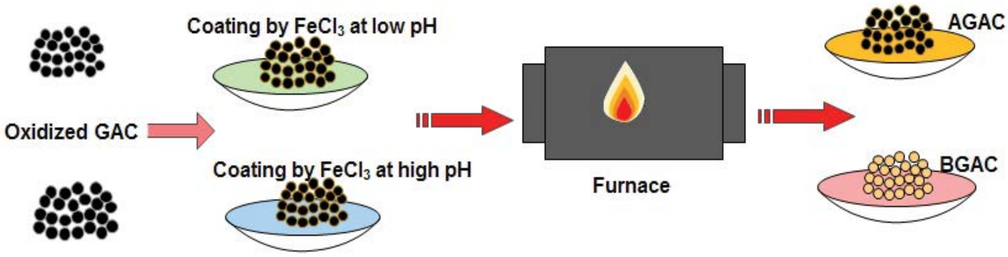

Fig. 1. The scheme of oxidized GAC modification in this study [28].

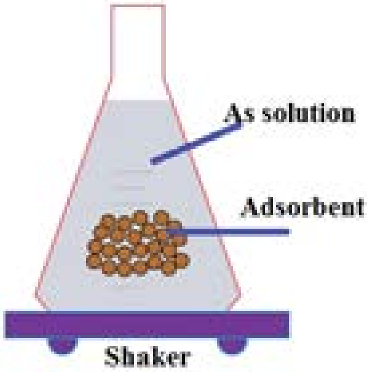

Fig. 2. The scheme of adsorption experiments as a batch method.

concentration, the kinetic studies, and adsorption isotherms. For optimum pH selection, 50 mL of arsenic solution (C_0 = 2.15 mg/L) introduced in 200 mL Erlenmeyer flasks. Then, 0.1 g of the adsorbents was put in contact with 50 mL of arsenic solution (dose of adsorbent was 2 g/L). The pH of the solutions was adjusted to 2, 3, 4, 6, 7, 8, and 10 by using 1 M HCl or 1 M NaOH. The samples were placed in mechanical shaker for 24 h at the room temperature (20°C ± 1°C) and the agitation speed of the shaker was fixed at 250 rpm for all batch experiments. After that, the combination of arsenic solution and adsorbents was filtered through Whatman paper (0.45 μm). The filtrate was preserved by reducing the pH ≤ 2 with 6 N HNO_3 for arsenate analysis. Finally, the residue concentration of arsenate was determined by ICP-MS (PerkinElmer, model ELAN DRC-e, USA). The adsorption kinetic study and equilibrium time were performed for As(V) solution at determined optimum pH and room temperature. For this section several Erlenmeyer flasks used to hold 50 mL As(V) solution with an initial concentration of 2.15 mg/L and 2 g/L of adsorbent. Samples agitated at 250 rpm for a duration ranging from 5 min to 24 h in 16 intervals. To obtain adsorption equilibrium isotherms, the effect of dose and concentration of arsenate, several initial concentrations of arsenate (0.3, 1.2, and 2.15 mg/L), and several doses of adsorbents (0.1, 0.5, 1, and 2 g/L) were used at determined optimum pH and contact time.

Percentage removal of As(V) and adsorption capacity of adsorbent at time t (q_t) were calculated as Eqs. (2) and (3):

$$\text{Percentage removal }\% = \left[1 - \frac{C_e}{C_0}\right] \times 100 \qquad (2)$$

where C_0 and C_e (mg/L) are the initial and equilibrium solute concentrations, respectively.

$$q_e\left(\text{mg}/\text{g}\right) = \left[\frac{C_0 - C_e}{M}\right] \times V \qquad (3)$$

where C_0 and C_e (mg/L) are the initial and final concentration of As(V) at time t in the solutions, respectively, M (g) is the amount of the adsorbent used, and V (L) is the volume of As(V) solution.

2.7. Characterization of the raw and modified GAC

The Brunauer–Emmett–Teller (BET) specific surface area and pore volumes of adsorbents before and after loading iron oxide were obtained by N_2 adsorption at 77 K with a Micromeritics 2000 instrument (ASAP 2000, Micromeritics, USA). The major chemical compositions of adsorbents and the morphologies of them were analyzed by X-ray diffraction (XRD) (Shimadzu, Japan, using graphite monochromatic copper radiation over the 2θ range 10°–80°) and scanning electron microscopy (SEM), respectively. SEM conducted by Holland Philips, JSM-5800. XRD pattern was taken from a Cu target X-ray diffractometer (Rigaku D/max-r B).

3. Results and discussion

3.1. Characterization of the raw and modified GAC

3.1.1. Surface area and pore properties

Iron content, the BET surface area and other related data about the raw and modified GAC and are shown in Table 1.

It can be seen that bay modification of GAC with $FeCl_3$, total volume, surface area, and total pore volume was decreased. These parameters were found to be in the order of raw GAC > AGAC > BGAC. Also, it was observed that Fe content of modifies GAC under acidic condition (AGAC) is more than modifies GAC under basic condition (BGAC). Under acidic condition Fe is mainly present as soluble so, it was penetrated in deep pore structure than the basic condition that Fe predominant as an insoluble. Under high pH, Fe precipitated on GAC surface so, the amounts of coating (iron contents) were smaller than modification under low pH (Table 1). Under low pH most of Fe goes through micro and macropores of GAC. When it was placed in a furnace for calcination at 300°C, most of Fe^{2+} fixed into pore space. At high pH condition most of soluble Fe precipitated on

Table 1
BET results for raw GAC and modified GAC (AGAC and BGAC)

Adsorbent samples	Total volume (cm^3/g)	BET surface area (m^2/g)	Total pore volume (cm^3/g)	Fe content (mg/g)
GAC	217.09	944.89	0.4621	2.5
AGAC	152.27	662.76	0.3326	156
BGAC	136.43	593/81	0.3114	81.2

GAC, so, it is not a chance for Fe to penetrate into micro pore. For this reason, the iron content of AGAC is greater than BGAC. The decrease in specific total volume, surface area, and total pore volume were mostly related to Fe precipitation and finally pore blockage and filling with Fe. Similar results were reported by another researcher. They have stated that oxidation and impregnation cause decreasing both surface areas and pores volume due to partial or complete pore blockage [21,30].

3.1.2. Morphology studies

Fig. 3 shows the SEM images of raw and modified GAC. It could be found that macropores in raw GAC are greater than AGAC and BGAC. Also, it was observed that Fe precipitation on BGAC surface is more than AGAC surface. May be it is related to this fact that in high pH Fe cations precipitated very quickly in the surface of GAC.

3.2. XRD studies

XRD patterns of the samples are shown in Fig. 4. It was founded that for raw GAC (Fig. 4(a)). Most of peaks are related to SiO_2 and graphite, this result is in accordance with Chen study. However, other XRD peaks are observed at around 2 h = 5°, 12°, 14°, 24°, and 25° that related to sodium silicates and sodium aluminum silicates. XRD results for modified GAC by $FeCl_3$ under acidic condition (AGAC) show that most of the peaks are related to Fe_2O_3 (maghemite), Fe_3O_4 (magnetite), and SiO_2 which were reported by another researcher, as well. Other XRD peaks are observed at around 2 h = 15°, 19°, 20°, 25°, 30°, and 45° that related to calcium aluminum silicate (Fig. 4(b)). For modified GAC by $FeCl_3$ under basic condition (BGAC) results show that most of the peaks are related to Fe_3O_4 (magnetite) and hydrogen aluminum silicate (Fig. 4(c)). Other XRD peaks are observed at around 2 h = 19°, 34°, 40°, 61°, 62°, and 69° which were related to calcium iron oxide. In this study, it was found that coating of GAC with $FeCl_3$ under acidic condition produced maghemite and magnetite, but for modified GAC with $FeCl_3$ under basic condition magnetite was predominant. This result related to this matter that under acidic condition (low pH) most of Fe presented as Fe^{2+} and when it was calcined under the controlled condition of N_2 gas, it changed to maghemite. On the other hand, under basic condition most of Fe presented as Fe^{3+} and when reacting with oxygen it precipitated as magnetite (Fe_3O_4). The previous study showed that Fe_3O_4 deposited on the surface of the carbon [31]. According to SEM and XRD results in this study, we had more deposit of Fe_3O_4 on BGAC surface. Also, empirical observation showed that the surface of BGAC has brown to yellow color.

3.3. Effect of pH on As(V) adsorption

One of the most important parameters in water and wastewater treatment process is pH. It can change the mechanism of all pollutants removal [8,32]. Also, for arsenic removal by adsorption, pH plays an important role because predominant species of As changed along with any change in

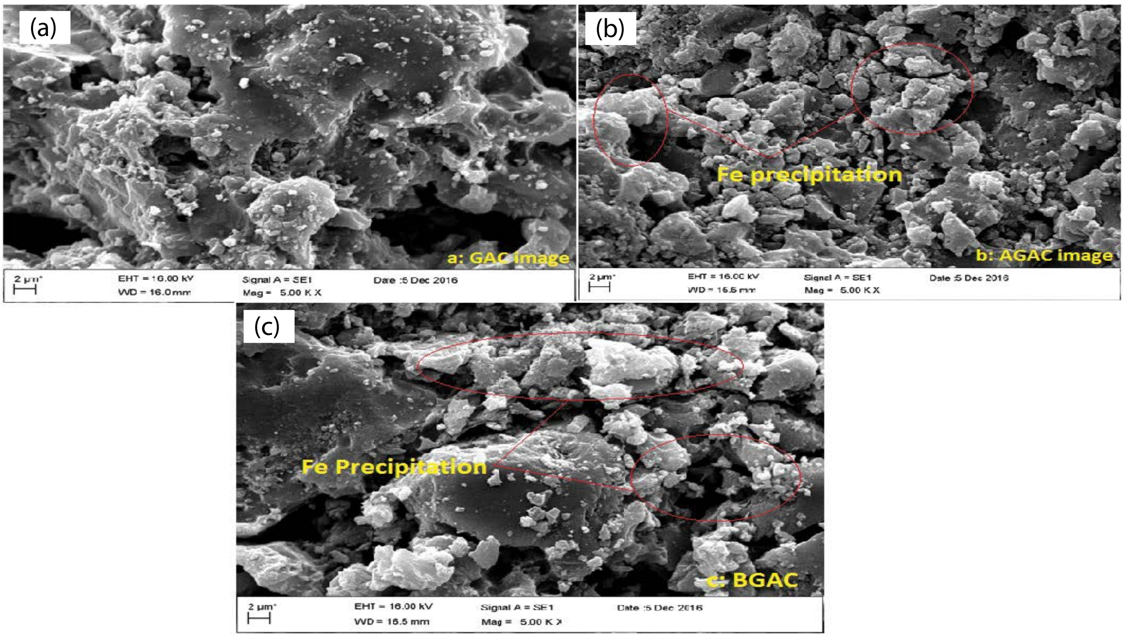

Fig. 3. SEM images of GAC (a), AGAC (b), and BGAC (c).

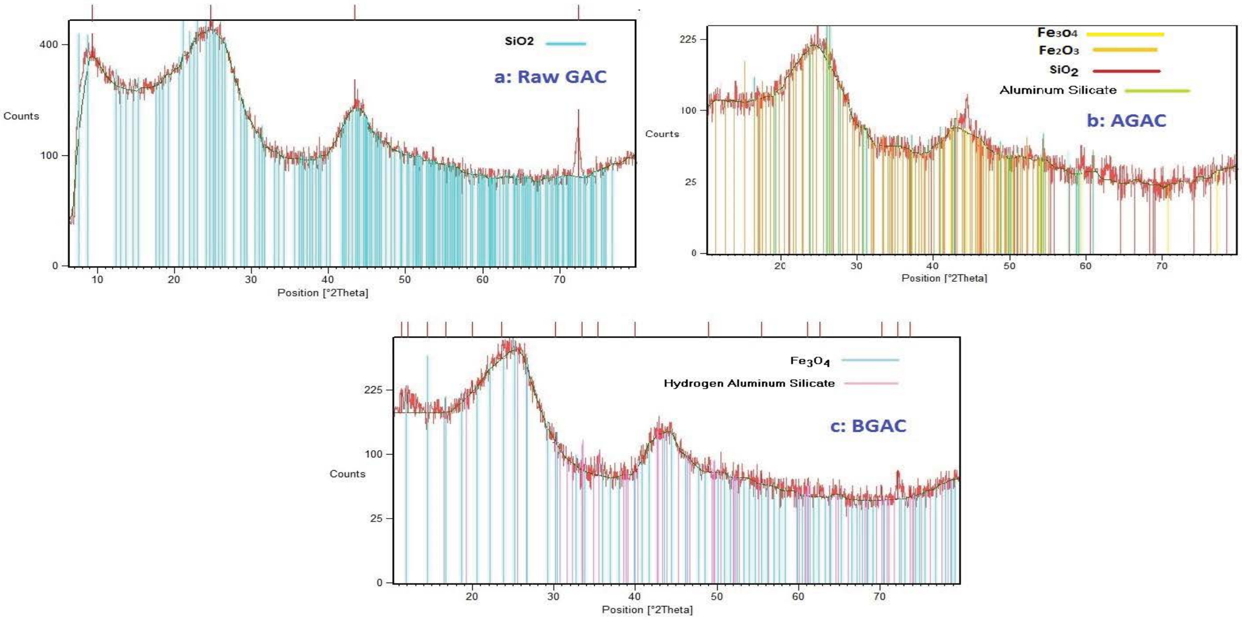

Fig. 4. XRD patterns of raw GAC (a), iron-loaded GAC after impregnation with iron (III) chloride under acidic condition, AGAC (b), and iron-loaded GAC after impregnation with iron (III) chloride under basic condition, BGAC (c).

pH value. For example, at pH 0–2 As(V) exists as H_3ASO_4, at pH 3–6 exists as $H_2ASO_4^{-2}$, and exists as $HASO_4^{-2}$ at pH 7–11 [33,34]. Therefore, for determination of pH effects on arsenic removal various pH values from 2 to 10 was studied (Fig. 5). From Fig. 3 it can be seen that removal efficiency of As(V) depended on the pH of the solution. The percentage of arsenic removal by AGAC was >90% throughout the pH range of 6–8. Also, for BGAC and raw GAC were 76%–86% and 62.8%–78.6%, respectively. The highest removal efficiency has taken place at pH = 8 so, it was chosen as an optimum pH condition for further experiments.

In this study, the results showed that arsenic removal efficiencies were increased by increasing of pH value from 2 to 8. As the pH is further increased, the adsorption capacity and removal efficiency decreased. Same results reported by Zhengang [31].

Main mechanism for the majority of adsorption process is affinity adsorption, but for modified adsorbents especially modified GAC with $FeCl_3$ chemical reaction with Fe_3O_4 play an important role for As(V) removal. The removal efficiency of As by AGAC was greater than BGAC because AGAC contains both Fe_2O_3 and Fe_3O_4 but BGAC contains only Fe_3O_4, so, it helped to adsorbed more arsenic. The maximum adsorption capacity of arsenic for AGAC, BGAC, and raw GAC at pH = 8 was 1.04, 0.93, and 0.85 mg/g, respectively. It can imply this matter that by adding 156 mg of iron to 1 g of GAC, adsorption capacity increased by about 0.19 mg in comparison with raw GAC.

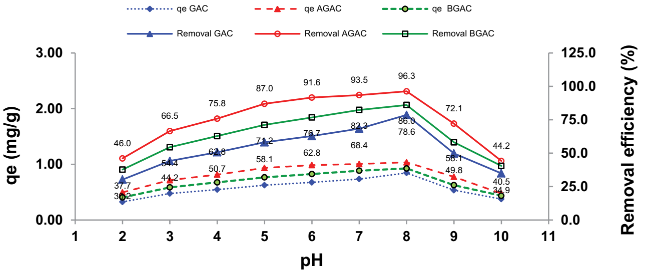

Fig. 5. Effect of pH on As(V) adsorption capacity and removal efficiency.

3.4. Effect of contact time

The effect of contact time on As(V) adsorption efficiency is shown in Fig. 6. It can be seen that the removal efficiency of As(V) onto the adsorbents significantly increases during the initial adsorption period of 3 h. Then, the removal of As(V) increased slowly and remained almost constant after 5 h. So, 5 h selected as an optimum contact time for further and next experiment. Other study reported same results and showed that removal rate of sorbate is rapid in initial time and it was gradually decreases with time until it reaches to equilibrium [35,36]. One reason for this event is that at the initial period

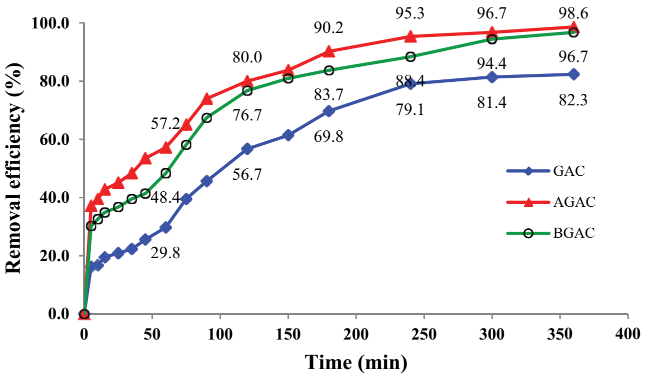

Fig. 6. Effect of contact time on As(V) adsorption efficiency.

of adsorption there are large numbers of vacant surface sites that available for adsorption. After a lapse of time, these sites occupied by As(V) so, the removal efficiency was decreased [37]. In this study, after 1 h the removal efficiency of As(V) by raw GAC, BGAC, and AGAC was 29.77%, 48.37%, and 57.21%, respectively. After 2 h it reached 56.74%, 76.74%, and 80%, respectively. Also, after 3 h it reached 69.77%, 83.72%, and 90.23%, respectively. Finally, at optimum time (5 h) it reached 81.4%, 94.42%, and 96.74%, respectively.

3.5. Kinetic study

The linear mathematical forms of the pseudo-first-order and pseudo-second-order equations [38] of kinetics used as below:

$$\text{Pseudo-first-order equation}: \log\left(q_e - q_t\right) = \log\left(q_e\right) - \frac{k_1}{2.303} \times t \quad (4)$$

$$\text{Pseudo-second-order equation}: \frac{t}{q_t} = \left(\frac{1}{k_2 q_e^2}\right) + \left(\frac{t}{q_e}\right) \quad (5)$$

where q_t is the amount of adsorbed contaminant (mg/g) at time t, q_e is the maximum adsorption capacity (mg/g) for the pseudo-first-order adsorption and pseudo-second-order adsorption, k_1 is the pseudo-first-order rate constant for the adsorption process (1/min), and k_2 is the pseudo-second-order rate constant (g/mg min). The sorption modeling parameters are summarized in Table 2.

Table 2 shows the kinetic parameters and the correlation coefficient (R^2) derived from the application of the pseudo-first-order and pseudo-second-order equations to the adsorption data of raw GAC, AGAC, and BGAC. The results show that for raw GAC and BGAC kinetics study fits with the pseudo-first-order with correlation coefficients of 0.97 and 0.99, respectively, and for AGAC it was fitted with pseudo-second-order with correlation coefficients of 0.98. The amounts of q_e for raw GAC, AGAC, and BGAC were 0.9, 0.98, and 0.86 mg/g, respectively.

Table 2
The kinetic sorption modeling parameters of As(V) on raw GAC, AGAC, and BGAC

Model	Parameters	Raw GAC	AGAC	BGAC
Pseudo-first-order	k_1 (1/min)	0.008	0.01	0.009
	q_e (mg/g)	0.9	0.8	0.86
	R^2	0.97	0.27	0.99
Pseudo-second-order	k_2 (1/min)	0.009	0.025	0.018
	q_e (mg/g)	1.12	1.15	1.14
	R^2	0.91	0.98	0.97

Initial concentration = 2.15 mg/L; adsorbents dose = 2 g/L.

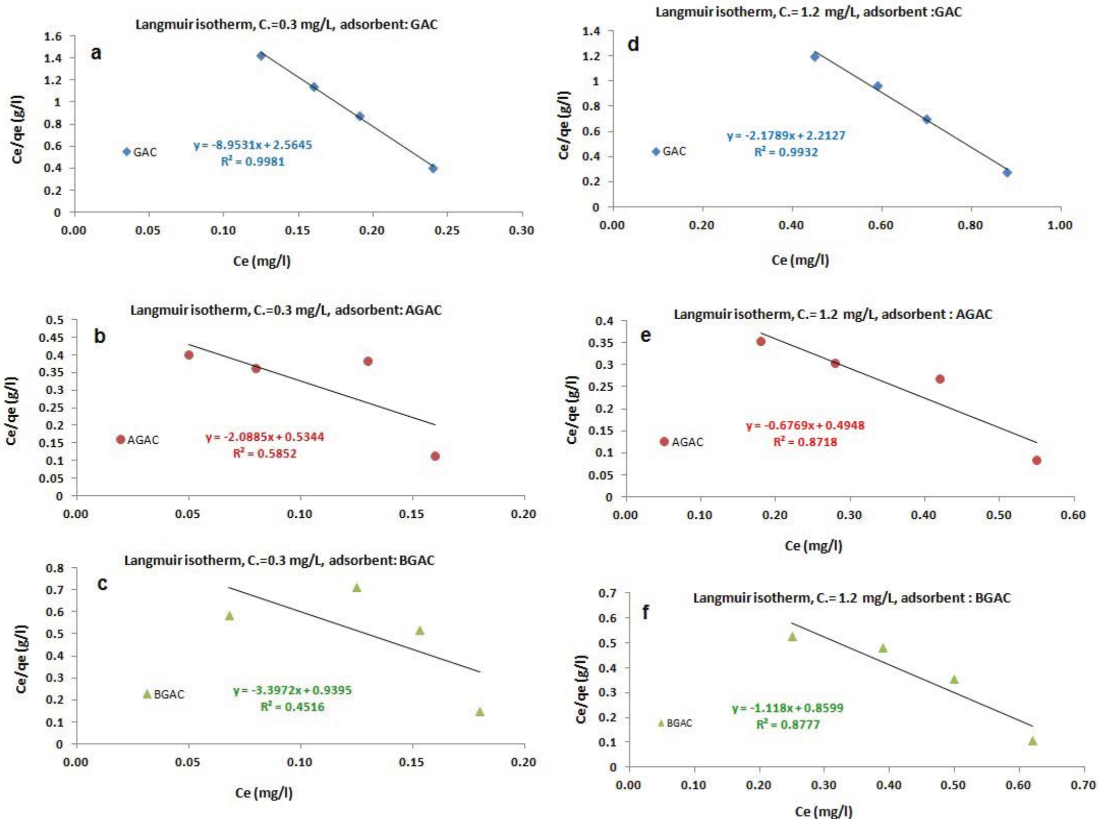

Fig. 7. (a)–(c) Langmuir isotherm (As(V) concentration was 0.3 mg/L, adsorbents dose: 0.1, 0.5, 1, and 2 g/L). (d)–(f) Langmuir isotherm (As(V) concentration was 1.2 mg/L, adsorbents dose: 0.1, 0.5, 1, and 2 g/L).

The previous study revealed that homogeneous cover of iron oxide on the adsorbent surface in comparison with large aggregates of iron oxide leads to equilibrium that much faster [39]. However, a larger *k* value (AGAC > BGAC > raw GAC) suggests that adsorption happened at the shorter time to reach equilibrium or As(V) uptake. In this study, same results obtained for AGAC compared with BGAC. Same kinetics of pseudo-second-order model was suggested by Vitela-Rodriguez for As(V) removal with modified ACs with iron hydroxide [40]. Some study claimed that pseudo-second-order kinetic was based on the assumption that the rate limiting step may be chemical sorption or chemisorptions including valency forces through sharing or exchange of electron between adsorbent and adsorbate [41].

3.6. Adsorption isotherms

In order to study the adsorption behavior of the As(V) ions on the adsorbents, the experimental data were fitted to Langmuir and Freundlich isotherm equation. Langmuir isotherm (Eq. (6)) says that adsorption takes place onto the homogeneous surface with a specific number of equivalent sites but, Freundlich isotherm (Eq. (7)) related to the sorption onto the heterogeneous surface [42].

$$\frac{C_e}{q_e} = \frac{1}{bq_m} + \frac{C_e}{q_m} \tag{6}$$

$$\log q_e = \log k_f + \frac{1}{n}\left(\log C_e\right) \tag{7}$$

where q_e and C_e represent the amount of As(V) adsorbed at equilibrium (mg/L) and the concentration at equilibrium (mg/L), respectively. The Langmuir constant, *b*, related to the binding energy and the maximum adsorption capacity (q_m). It can be determined from the intercept and the slope of the linear plot between C_e/q_e and C_e.

The Langmuir and Freundlich isotherm for As(V) adsorption with raw GAC, AGAC, and BGAC are presented in Figs. 7 and 8. Also, adsorption isotherm parameters and correlation coefficients (R^2) for As(V) adsorption are given in Table 3. Based on R^2 values, the adsorption of As(V) by raw GAC has been well described by the Langmuir model. In contrast the adsorption of As(V) by AGAC and BGAC has been well described by the Freundlich model. It implies that for raw GAC, adsorption is limited to a monolayer, but for AGAC and BGAC adsorption is not limited to a monolayer. On the other hand As(V) molecules migrate to heterogeneous surfaces of

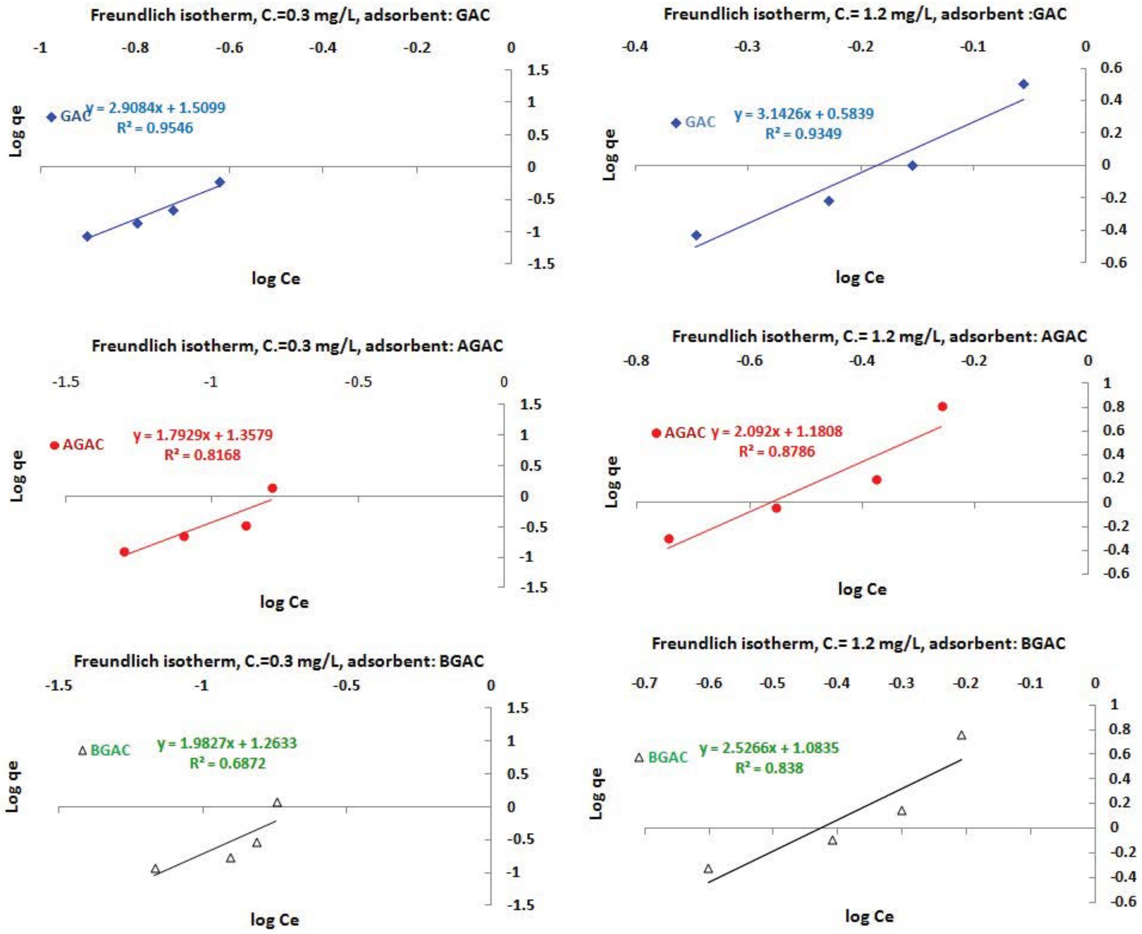

Fig. 8. (a)–(c) Freundlich isotherm (As(V) concentration was 0.3 mg/L, adsorbents dose: 0.1, 0.5, 1, and 2 g/L). (d)–(f) Freundlich isotherm (As(V) concentration was 1.2 mg/L, adsorbents dose: 0.1, 0.5, 1, and 2 g/L).

Table 3
The Langmuir and Freundlich parameters and correlation coefficients for As(V) adsorption onto raw GAC, AGAC, and BGAC

Model	Initial concentration (mg/L)	Parameters	Raw GAC	AGAC	BGAC
Langmuir	0.3	b (l/mg)	3.49	3.9	3.6
		q_m (mg/g)	0.11	0.47	0.29
		R^2	**0.99**	0.58	0.48
	1.2	b (l/mg)	0.98	1.36	0.89
		q_m (mg/g)	0.45	1.47	1.3
		R^2	**0.99**	0.87	0.8
Freundlich	0.3	$1/n$	2.9	1.79	1.98
		k_f (mg/g)	14.35	22.7	18.33
		R^2	0.95	**0.81**	**0.68**
	1.2	$1/n$	3.14	2.09	2.5
		k_f (mg/g)	3.83	15.1	12.12
		R^2	0.93	**0.878**	**0.83**

Initial concentration = 1.2 and 0.3 mg/L; adsorbents dose = 0.1, 0.5, 1, and 2 g/L.

AGAC and BGAC that following the Freundlich isotherm theory but for raw GAC the adsorption of the metal ions occurs on a homogeneous surface (Langmuir model assumption).

One indicator that can be used for determining of the favorability of adsorption with Freundlich model is the magnitude of the Freundlich exponent (n). Exponent values between $1 < n < 10$ show a beneficial adsorption [43]. Of course, in this study the parameter for this study was below one but correlation coefficients helped us to select the best isotherm that mentioned in the previous section. Another study was suggested pseudo-second-order model for As(V) adsorption by an iron oxide/AC. The adsorption capacity of AGAC according to Freundlich isotherms (k_f) for 0.3 and 1.2 mg/L of As(V) was 22.7 and 15.1 mg/g, respectively, and for BGAC was 18.33 and 12.12 mg/g, respectively. The adsorption capacity of raw GAC according to Langmuir isotherms (q_m) for 0.3 and 1.2 mg/L of As(V) was 0.11 and 0.45 mg/g, respectively. So, Langmuir isotherms showed that the adsorption capacity increases with increasing concentration of As(V), but Freundlich isotherms showed that the adsorption capacity decreased with increasing concentration of As(V). The results of this study are promising and are comparative with heavy metal removal with other similar processes [44].

4. Conclusions

In this study, it was concluded that modified GAC with $FeCl_3$ under acidic condition contains maghemite and magnetite (Fe_2O_3 and Fe_3O_4) but for modified GAC under basic condition it only contained magnetite (Fe_3O_4). The iron content of modified GAC with $FeCl_3$ under acidic condition is more than modified GAC under the basic condition. BET analysis showed that by modifying of GAC with $FeCl_3$ the specific total volume, surface area, and total pore volume were decreased. Removal of arsenic reached equilibrium after 5 h. The As(V) adsorption increased with increasing pH until pH 8 and maximum adsorption was obtained at pH 8. Increasing the Fe content of modified GAC increases the arsenic uptake. The performances of the AGAC and BGAC adsorbents were compared with raw GAC showed fast adsorption kinetics as well as high adsorption capacities. Arsenic adsorption with modified GAC (AGAC and BGAC) fitted with Freundlich model while raw GAC fitted with Langmuir model.

Acknowledgements

The authors acknowledge the fund provided by the Isfahan University of Medical Science, School of Health, and Environmental Health Engineering Department of Isfahan – Iran for this PhD thesis with 394281 code number. Also, the authors would like to give special thanks to Department of Environmental Health Engineering of Saveh University of Medical Science, Isfahan Water & Wastewater Company, and National Water & Wastewater Company of Iran for all cooperation.

References

[1] A. Maiti, J.K. Basu, S. De, Experimental and kinetic modeling of As(V) and As(III) adsorption on treated laterite using synthetic and contaminated groundwater: effects of phosphate, silicate and carbonate ions, Chem. Eng. J., 191 (2012) 1–12.

[2] M. Ciopec, A. Negrea, L. Lupa, C. Davidescu, P. Negrea, P. Sfârloaga, Performance evaluation of the Fe-IR-120 (Na)-DEHPA impregnated resin in the removal process of As(V) from aqueous solution, J. Mater. Sci. Eng., B, 1 (2011) 421.

[3] M. Mahdavi, M.M. Amin, A.H. Mahvi, H. Pourzamani, A. Ebrahimi, Metals, heavy metals and microorganism removal from spent filter backwash water by hybrid coagulation-UF processes, J. Water Reuse Desal., 8 (2018) 225–233.

[4] A. Goswami, P. Raul, M. Purkait, Arsenic adsorption using copper (II) oxide nanoparticles, Chem. Eng. Res. Des., 90 (2012) 1387–1396.

[5] Z. Atafar, A. Mesdaghinia, J. Nouri, M. Homaee, M. Yunesian, M. Ahmadimoghaddam, A.H. Mahvi, Effect of fertilizer application on soil heavy metal concentration, Environ. Monit. Assess., 160 (2010) 83.

[6] J. Nouri, A. Mahvi, G. Jahed, A. Babaei, Regional distribution pattern of groundwater heavy metals resulting from agricultural activities, Environ. Geol., 55 (2008) 1337–1343.

[7] R. Harisha, K. Hosamani, R. Keri, S. Nataraj, T. Aminabhavi, Arsenic removal from drinking water using thin film composite nanofiltration membrane, Desalination, 252 (2010) 75–80.

[8] A. Ebrahimi, M.M. Amin, H. Pourzamani, Y. Hajizadeh, A.H. Mahvi, M. Mahdavi, M.H.R. Rad, Hybrid coagulation-UF processes for spent filter backwash water treatment: a comparison studies for PAFCl and $FeCl_3$ as a pre-treatment, Environ. Monit. Assess., 189 (2017) 189–387.

[9] T. Türk, I. Alp, Arsenic removal from aqueous solutions with Fe-hydrotalcite supported magnetite nanoparticle, J. Ind. Eng. Chem., 20 (2014) 732–738.

[10] R. Ebrahimi, A. Maleki, B. Shahmoradi, H. Daraei, A.H. Mahvi, A.H. Barati, A. Eslami, Elimination of arsenic contamination from water using chemically modified wheat straw, Desal. Wat. Treat., 51 (2013) 2306–2316.

[11] E. Bazrafshan, H. Faridi, F.K. Mostafapour, A.H. Mahvi, Removal of arsenic from aqueous environments using *Moringa peregrina* seed extract as a natural coagulant, Asian J. Chem., 25 (2013) 3557–3561.

[12] H. Farrokhzadeh, E. Taheri, A. Ebrahimi, A. Fatehizadeh, M.V. Dastjerdi, B. Bina, Effectiveness of *Moringa oleifera* powder in removal of heavy metals from aqueous solutions, Fresenius Environ. Bull., 22 (2013) 1516–1523.

[13] A. Abdolahnejad, N. Jafari, A. Ebrahimi, A. Mohammadi, H. Farrokhzadeh, Removal of arsenic and coliform bacteria by modified sand filter with slag and zeolite from drinking water. Health Scope, 6 (2017) 1–7.

[14] B.Z. Can, R. Boncukcuoglu, A.E. Yilmaz, B.A. Fil, Effect of some operational parameters on the arsenic removal by electrocoagulation using iron electrodes, J. Environ. Health Sci. Eng., 12 (2014) 95.

[15] A. Dominguez-Ramos, K. Chavan, V.n. García, G. Jimeno, J. Albo, K.V. Marathe, G.D. Yadav, A. Irabien, Arsenic removal from natural waters by adsorption or ion exchange: an environmental sustainability assessment, Ind. Eng. Chem. Res., 53 (2014) 18920–18927.

[16] F. Hesami, B. Bina, A. Ebrahimi, M.M. Amin, Arsenic removal by coagulation using ferric chloride and chitosan from water, Int. J. Environ. Health Eng., 2 (2013) 17.

[17] A. Ebrahimi, M.M. Amin, Y. Hajizadeh, H. Pourzamani, M. Memarzadeh, A.H. Mahvi, M. Mahdavi, Filter backwash water treatment by coagulation: a comparison study by polyaluminium ferric chloride and ferric chloride, Desal. Wat. Treat., 66 (2017) 320–329.

[18] R. Li, Q. Li, S. Gao, J.K. Shang, Exceptional arsenic adsorption performance of hydrous cerium oxide nanoparticles: Part A. Adsorption capacity and mechanism, Chem. Eng. J., 185 (2012) 127–135.

[19] G. Zhang, Z. Ren, X. Zhang, J. Chen, Nanostructured iron (III)-copper (II) binary oxide: a novel adsorbent for enhanced arsenic removal from aqueous solutions, Water Res., 47 (2013) 4022–4031.

[20] Y. Salameh, A.B. Albadarin, S. Allen, G. Walker, M. Ahmad, Arsenic (III, V) adsorption onto charred dolomite: charring optimization and batch studies, Chem. Eng. J., 259 (2015) 663–671.

[21] A. Yürüm, Z.Ö. Kocabaş-Ataklı, M. Sezen, R. Semiat, Y. Yürüm, Fast deposition of porous iron oxide on activated carbon by microwave heating and arsenic (V) removal from water, Chem. Eng. J., 242 (2014) 321–332.

[22] Q.L. Zhang, Y. Lin, X. Chen, N.Y. Gao, A method for preparing ferric activated carbon composites adsorbents to remove arsenic from drinking water, J. Hazard. Mater., 148 (2007) 671–678.

[23] Z. Gu, J. Fang, B. Deng, Preparation and evaluation of GAC-based iron-containing adsorbents for arsenic removal, Environ. Sci. Technol., 39 (2005) 3833–3843.

[24] G. Muniz, V. Fierro, A. Celzard, G. Furdin, G. Gonzalez-Sánchez, M. Ballinas, Synthesis, characterization and performance in arsenic removal of iron-doped activated carbons prepared by impregnation with Fe(III) and Fe(II), J. Hazard. Mater., 165 (2009) 893–902.

[25] W. Chen, R. Parette, J. Zou, F.S. Cannon, B.A. Dempsey, Arsenic removal by iron-modified activated carbon, Water Res., 41 (2007) 1851–1858.

[26] P. Mondal, C. Balomajumder, B. Mohanty, A laboratory study for the treatment of arsenic, iron, and manganese bearing ground water using Fe^{3+} impregnated activated carbon: effects of shaking time, pH and temperature, J. Hazard. Mater., 144 (2007) 420–426.

[27] Z. Li, Q. Yang, Y. Zhong, X. Li, L. Zhou, X. Li, G. Zeng, Granular activated carbon supported iron as a heterogeneous persulfate catalyst for the pretreatment of mature landfill leachate, RSC Adv., 6 (2016) 987–994.

[28] M. Mahdavi, A. Ebrahimi, A.H. Mahvi, A. Fatehizadeh, F. Karakani, H. Azarpira, Experimental data for aluminum removal from aqueous solution by raw and iron-modified granular activated carbon, Data Brief, 17 (2018) 731–738.

[29] Q. Chang, W. Lin, W.-c. Ying, Preparation of iron-impregnated granular activated carbon for arsenic removal from drinking water, J. Hazard. Mater., 184 (2010) 515–522.

[30] M.M. Maroto-Valer, I. Dranca, T. Lupascu, R. Nastas, Effect of adsorbate polarity on thermodesorption profiles from oxidized and metal-impregnated activated carbons, Carbon, 42 (2004) 2655–2659.

[31] Z. Liu, F.S. Zhang, R. Sasai, Arsenate removal from water using Fe_3O_4-loaded activated carbon prepared from waste biomass, Chem. Eng. J., 160 (2010) 57–62.

[32] A. Ebrahimi, E. Taheri, A. Pashaee, M. Mahdavi, The effectiveness of polyaluminum ferric chloride (PAFCl) for turbidity and color removal from Isfahan raw water, Desal. Water Treat., 55 (2015) 1966–1972.

[33] Y. Chammui, P. Sooksamiti, W. Naksata, S. Thiansem, O.-A. Arqueropanyo, Removal of arsenic from aqueous solution by adsorption on leonardite, Chem. Eng. J., 240 (2014) 202–210.

[34] J. Youngran, F. Maohong, J. Van Leeuwen, J.F. Belczyk, Effect of competing solutes on arsenic (V) adsorption using iron and aluminum oxides, J. Environ. Sci., 19 (2007) 910–919.

[35] O. Gulnaz, A. Sahmurova, S. Kama, Removal of Reactive Red 198 from aqueous solution by *Potamogeton crispus*, Chem. Eng. J., 174 (2011) 579–585.

[36] F. Kord Mostafapour, E. Bazrafshan, M. Farzadkia, S. Amini, Arsenic removal from aqueous solutions by *Salvadora persica* stem ash, J. Chem., 2013 (2012) 1–8.

[37] S. Yao, Z. Liu, Z. Shi, Arsenic removal from aqueous solutions by adsorption onto iron oxide/activated carbon magnetic composite, J. Environ. Health Sci. Eng., 12 (2014) 58.

[38] A. El Nemr, Potential of pomegranate husk carbon for Cr (VI) removal from wastewater: kinetic and isotherm studies, J. Hazard. Mater., 161 (2009) 132–141.

[39] Z.Ö. Kocabaş-Ataklı, Y. Yürüm, Synthesis and characterization of anatase nanoadsorbent and application in removal of lead, copper and arsenic from water, Chem. Eng. J., 225 (2013) 625–635.

[40] A.V. Vitela-Rodriguez, J.R. Rangel-Mendez, Arsenic removal by modified activated carbons with iron hydro (oxide) nanoparticles, J. Environ. Manage., 114 (2013) 225–231.

[41] Y.-S. Ho, G. McKay, The kinetics of sorption of divalent metal ions onto sphagnum moss peat, Water Res., 34 (2000) 735–742.

[42] T. Phuengprasop, J. Sittiwong, F. Unob, Removal of heavy metal ions by iron oxide coated sewage sludge, J. Hazard. Mater., 186 (2011) 502–507.

[43] R. Treybal, Mass Transfer Operations, McGraw-Hill, New York, 1980.

[44] H.J. Mansoorian, A.H. Mahvi, A.J. Jafari, Removal of lead and zinc from battery industry wastewater using electrocoagulation process: influence of direct and alternating current by using iron and stainless steel rod electrodes, Sep. Purif. Technol., 135 (2014) 165–175.